JOURNAL OF AEROSPACE COMPUTING, INFORMATION, AND COMMUNICATION
Vol. 6, March 2009

Aerodynamic Multiobjective Design Exploration of a Flapping Airfoil Using a Navier–Stokes Solver

Akira Oyama*
Institute of Space and Astronautical Science, Japan Aerospace Exploration Agency, Sagamihara, Kanagawa, 229-8510, Japan

Yoshiyuki Okabe† and Koji Shimoyama‡
University of Tokyo, Sagamihara, Kanagawa, 229-8510, Japan

and

Kozo Fujii§
Institute of Space and Astronautical Science, Japan Aerospace Exploration Agency, Sagamihara, Kanagawa, 229-8510, Japan

DOI: 10.2514/1.35992

Aerodynamic knowledge for flapping airfoil is obtained by application of the multiobjective design exploration framework to a multiobjective aerodynamic flapping airfoil design optimization problem. The objectives of the design optimization problem are 1) time-averaged lift coefficient maximization, 2) time-averaged drag coefficient minimization, and 3) time-averaged required power coefficient where the airfoil oscillates in plunging and pitching modes. Pareto-optimal solutions are obtained by a multiobjective evolutionary optimization and analyzed with the self-organizing map. Aerodynamic performance of each flapping airfoil is evaluated by a two-dimensional Navier–Stokes solver. Analysis of the flow over the extreme Pareto-optimal flapping airfoils provides insights into flow mechanism for thrust maximization, lift maximization, and required power minimization. Analysis of the design objectives and design parameters with the self-organizing map leads to useful guidelines for practical flapping-wing micro air vehicles. The present result ensures that the multiobjective design exploration framework is useful approach for real-world design optimization problems.

Nomenclature

$C_{\mathrm{L}}(t)$	lift coefficient
$C_{\mathrm{M}}(t)$	moment coefficient
C_{p}	pressure coefficient

Received 3 December 2007; revision received 10 September 2008; accepted for publication 24 November 2008.

* Assistant Professor, Department of Space Transportation Engineering, 3-1-1 Yoshinodai, oyama2@flab.isas.jaxa.jp, Member AIAA.
† Graduate Student, Department of Aeronautics and Astronautics; currently, Mitsubishi Heavy Industries, Takasago Research & Development Center, 2-1-1, Shinhama, Araicho, okabe@flab.isas.jaxa.jp.
‡ Ph.D. candidate, Department of Aeronautics and Astronautics; currently, Research Fellow, Tohuku University, Institute of Fluid Science, 2-1-1 Katahira, Aoba, shimoyama@edge.ifs.tohoku.ac.jp, Member AIAA.
§ Professor, Department of Space Transportation Engineering, 3-1-1 Yoshinodai, fujii@flab.isas.jaxa.jp, Fellow AIAA.

$C_{PR}(t)$	required power coefficient
$C_T(t)$	thrust coefficient
c	airfoil chord
f	flapping frequency nondimensionalized with U_∞ and c
h	plunge amplitude nondimensionalized with c
k	reduced frequency, $2\pi f c/U_\infty$
St	Strouhal number, $kh/2\pi$
T	flapping period nondimensionalized with U_∞ and c
t	time nondimensionalized with U_∞ and c
U_∞	freestream velocity
$x(t)$	horizontal position nondimensionalized with c
$y(t)$	vertical position nondimensionalized with c
$\alpha(t)$	pitch angle
α_o	pitch angle offset
α_1	pitch angle amplitude
ϕ	phase shift
η	propulsive efficiency, C_T/C_{PR}
Subscript	
ave	time-averaged value over one flapping cycle

I. Introduction

RESEARCH interest in flapping wings in aerospace engineering has recently increased as flapping wing systems may be more suitable for micro air vehicles (MAVs) than fixed-wing systems at low Reynolds number. For the development of MAV with flapping wing systems, understanding of aerodynamic mechanism of a flapping wing for higher aerodynamic performance in terms of lift, thrust, and efficiency is important. Garrick [1] estimated the thrust and propulsive efficiency of plunging or pitching airfoils using incompressible potential flow analysis. He demonstrated that thrust is proportional to square of frequency and square of plunge amplitude. Tuncer and Platzer [2] performed Navier–Stokes computations of an oscillating airfoil, where the propulsive efficiency is found to be a strong function of reduced frequency and the plunge amplitude. Isogai et al. [3] performed a parametric study of an airfoil oscillating in coupled mode (pitching and plunging) using Navier–Stokes simulations, where the highest efficiency was achieved in 'the case in which the pitching oscillation advances 90 degrees ahead of the plunging oscillation and the reduced frequency is at some optimum value'. Tuncer and Kaya [4] optimized thrust and/or propulsive efficiency of an oscillating airfoil using a gradient-based method coupled with a Navier–Stokes solver where design parameters are pitch and plunge amplitudes and the phase shift between the pitch and plunge motions. They demonstrated that there is tradeoff between maximizations of thrust and propulsive efficiency and effective angle of attack is to be reduced for a high propulsive efficiency to prevent large-scale leading edge separation. Anderson et al. [5] experimentally showed that the phase angle shift between pitch and plunge oscillations have strong effects on propulsive efficiency.

While studies in the past have given significant insight into understanding the aerodynamic mechanism of a flapping wing, most of them considered only maximization of thrust and propulsive efficiency. Previous discussions on tradeoff between thrust and propulsive efficiency were intricate because propulsive efficiency is a function of the thrust itself. For example, higher thrust turns out to have higher propulsive efficiency even if the used power is constant. Thus, in addition to thrust, required power instead of propulsive efficiency should be considered for easier understanding of the flapping mechanism. Past studies also have not discussed the relationship between these aerodynamic performances and lift, which is an important aerodynamic index as it determines vehicle, payload, and fuel weights. In fact, the flapping motion design is a typical multiobjective design optimization problem that has three contradicting objectives; maximization of thrust, maximization of lift, and minimization of required power.

Recently, the idea of 'multiobjective design exploration (MODE)' was proposed as a tool to extract essential knowledge from multiobjective optimization problems such as tradeoff information between contradicting objectives and effects of each design parameter on the objectives. In the MODE framework, Pareto-optimal solutions are obtained

by using multiobjective optimizations such as multiobjective evolutionary algorithms [6] and then important design knowledge is extracted by analyzing the obtained Pareto-optimal solutions using so-called data mining approaches such as self-organizing map (SOM) [7] and analysis of variance [8]. Obayashi et al. applied the idea of MODE to understand fly-back booster of reusable launch vehicle design and regional-jet wing design and got some practically import design knowledge [9]. Here, multiobjective optimization and usage of data mining methods are essential parts of MODE. Pareto-optimal solutions contains such information as: which objectives are contradicting, which design parameters determine Pareto-optimal solutions/nonPareto-optimal solutions, which design parameters are related to the tradeoff between the objectives, and so on. If a single-objective optimization is done, obtaining such information is not straightforward. A typical multiobjective design optimization problem involves some objectives (sometimes more than ten) and dozens of design variables (sometimes more than a hundred). Usage of data mining methods is necessary to analyze Pareto-optimal solutions of such design problems.

The objective of the present study is to extract aerodynamic knowledge on the flapping motion such as 1) tradeoff information between lift, thrust, and required power, 2) effect of flapping motion parameters such as plunge amplitude and frequency, pitching angle amplitude and offset, and phase difference on the objective functions, and to create guidelines for the design of flapping motion for lift maximization, thrust maximization and required power minimization. To obtain such knowledge, the MODE framework is applied to a multiobjective aerodynamic design optimization problem of a flapping airfoil for a MAV for Mars exploration where lift and thrust are maximized and required power is minimized. The aerodynamic performance and required power are evaluated with the numerical simulations of the two-dimensional incompressible Navier–Stokes equations. Multiobjective evolutionary algorithm and self-organizing map are used to explore the design problem.

II. Design Optimization Problem

Entomopter, which is a MAV discussed in the United States for future Mars exploration [10,11], is considered. Entomopter has flapping wing system intending higher lift in extremely low atmospheric density at Mars surface (1/70 that at Earth surface) and take off, landing, and hovering capabilities. This MAV has a span length of 1 m and chord length of 0.1 m. The wing airfoil is thin with moderate camber and a sharp leading edge to enhance vortex generation. Its cruising speed is more than 10 km/h and flight time of a typical mission is 12 min. The cruising Reynolds number based on Mars air properties and reference length of the chord is assumed to be 10^3. It is estimated that the wing of Entomopter will produce lift coefficients between 7.95 and 10.6 with the help of boundary layer blowing. Note that the results are applicable to MAV on the earth because the Reynolds number is only the non-dimensional parameter that represents Mars atmosphere in this study.

As a first step towards understanding the flapping wing mechanism, a flapping airfoil is considered in this study. The objectives of the present design optimization problem are maximization of the time-averaged lift and thrust coefficients and minimization of the time-averaged required power coefficient at its cruising condition, where the lift, thrust, and required power are averaged over one flapping cycle:

$$C_{\mathrm{L,ave}} = f \cdot \int_{t=0}^{1/f} C_{\mathrm{L}}(t)\mathrm{d}t \tag{1}$$

$$C_{\mathrm{T,ave}} = f \cdot \int_{t=0}^{1/f} C_{\mathrm{T}}(t)\mathrm{d}t \tag{2}$$

$$C_{\mathrm{PR,ave}} = f \cdot \int_{t=0}^{1/f} C_{\mathrm{PR}}(t)\mathrm{d}t \tag{3}$$

where

$$C_{\mathrm{PR}}(t) = -\left(\frac{\mathrm{d}y(t)}{\mathrm{d}t} \cdot C_{\mathrm{L}}(t) + \frac{\mathrm{d}\alpha(t)}{\mathrm{d}t} \cdot C_{\mathrm{M}}(t)\right) \tag{4}$$

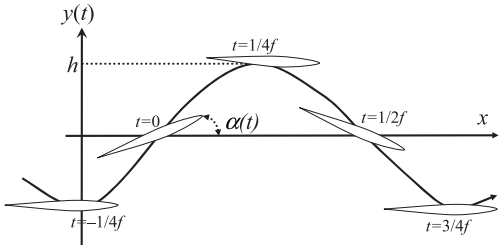

Fig. 1 Parameterization of flapping motion.

Table 1 Design space

Design parameters	Lower boundary	Upper boundary
Reduced frequency k	0.2	0.9
Plunge amplitude h	0.5	2.2
Pitch amplitude α_1	10 [deg]	45 [deg]
Pitch offset α_0	0 [deg]	30 [deg]
Phase shift ϕ	70 [deg]	110 [deg]

Constraints are applied on averaged lift and thrust coefficients so that they are positive. The airfoil is assumed to be NACA 0002 airfoil. The flapping motion of the airfoil (see Fig. 1) is expressed by plunging and pitching motions as:

$$x(t) = t \tag{5}$$

$$y(t) = h \cdot \sin(kt) \tag{6}$$

$$\alpha(t) = \alpha_1 \sin(kt + \phi) + \alpha_0 \tag{7}$$

where design parameters are h, k, α_0, α_1, and ϕ. The present design space is shown in Table 1.

III. Aerodynamic Force Evaluation

The two-dimensional incompressible Navier–Stokes equations and the continuity equation on the generalized curvilinear coordinates are solved using pseudo-compressible flow simulation approach [12]. The dual-time stepping procedure [13], which allows an implicit method to be used in real time with the updated solution obtained through subiterations in pseudo-time, is employed. The numerical fluxes are evaluated by the Roe scheme [14] where physical properties at the grid interface are evaluated by the MUSCL interpolation [15] based on primitive variables. The viscous terms are evaluated by second-order central differencing scheme. Lower-upper symmetric Gauss-Seidel (LU-SGS) factorization implicit algorithm [16] is used for the time integration. Note that the original version of the program for compressible flow analysis has been used for a wide variety of computational fluid dynamic (CFD) studies [17–19].

To compute aerodynamic performance of flapping motions, three cycles are simulated and averaged lift and thrust coefficients and required power are obtained for the third flapping cycle. Figure 2 shows the time history of lift coefficient of three flapping motions. This figure indicates that the lift coefficient is periodic and the lift coefficient for the second and third cycle is qualitatively same.

The corresponding computational grid is a C-type grid (Fig. 3) that has 201 (chordwise direction) $\times$101 (normal direction) grid size. Number of grid points on the airfoil is 151. Minimum spacing near the wall is 0.0001. Number of time steps for each flapping cycle is 1700. To confirm grid and time step size convergence, four computational results with different grid sizes and numbers of time steps in each flapping cycle are compared in Table 2. Time histories of C_{L} in the third flapping period are compared in Fig. 4. Because $C_{\mathrm{L,ave}}$ and maximum and minimum C_{L} are almost the same, it is concluded that the present grid size and time step size are enough for qualitative discussion.

The freestream flow conditions are applied to the inflow boundary. The outer boundary of the computational doman is placed at twenty chord lengths away from the leading edge of the airfoil. On the outflow boundary, pressure

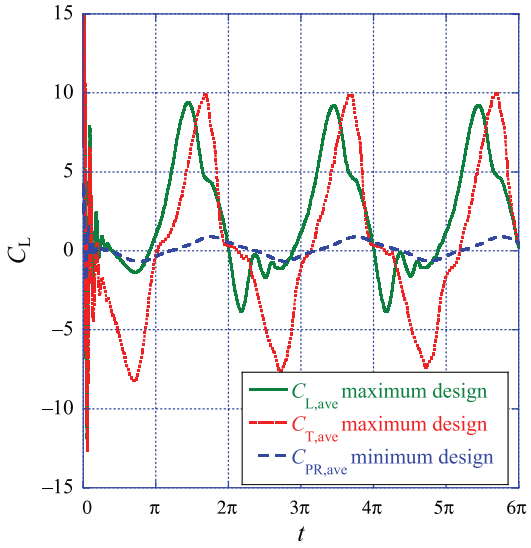

Fig. 2 Time histories of C_L.

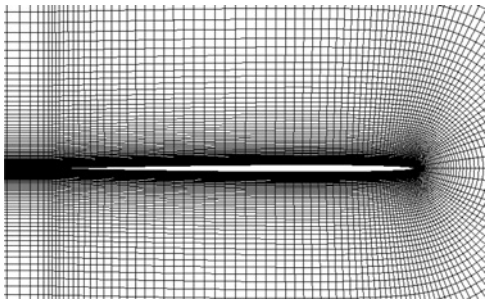

Fig. 3 Close-up view of the computational grid near the airfoil.

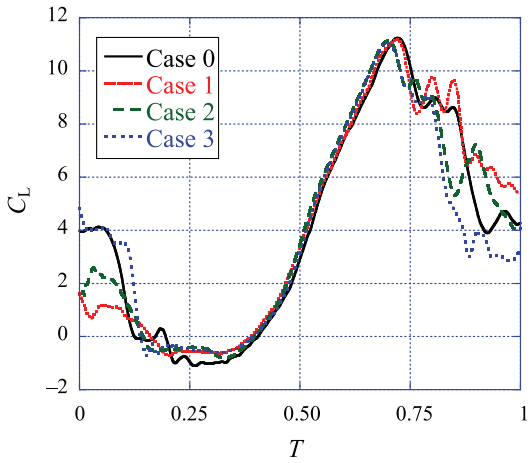

Fig. 4 Δx and Δt convergence.

Table 2 Number of grid points and time steps in each case

	Number of grid points	Number of time steps in each period	$C_{\mathrm{L,ave}}$
Case 0	201×101	1700	4.02
Case 1	401×201	3400	4.07
Case 2	401×201	6800	3.97
Case 3	401×201	13,600	3.79

is fixed to the freestream value while the other physical properties are extrapolated from the corresponding interior grid points. The airfoil surface is treated as a non-slip wall boundary. Physical properties on the wake boundary are interpolated from the adjacent grid points. The initial condition is the uniform flow.

IV. Design Optimization

The objective of the present study is to obtain aerodynamic knowledge for researchers or designers of flapping wing MAV from the multiobjective MAV design problem. To extract such knowledge, it is necessary to obtain Pareto-optimal solutions of the multiobjective design optimization problem and to analyze them with data mining approaches such as self-organizing maps.

Traditional methods such as gradient-based methods are basically single-objective optimization methods. When such a method is applied to a multiobjective optimization problem, the problem is converted to a single-objective design optimization problem by combining the multiple objectives into a single objective typically using a weighted sum method. This approach can find only one of the Pareto-optimal solutions corresponding to the user-specified weight coefficients. Hence, a multiobjective design optimization method is required for the present study.

Multiobjective evolutionary algorithm (MOEA, for example, see [6]) is an optimization algorithm mimicking mechanism of natural evolution, where a biological population evolves over generations to adapt to an environment by selection, recombination and mutation. MOEA has multiobjective optimization nature thanks to its population-based search algorithm toward higher fitness regions where fitness is determined through Pareto-ranking and fitness sharing. In addition, MOEA has some other advantages over traditional approaches such as:

1. Suitability to real-world design optimization problems: Because MOEA does not use function gradients, MOEA is suitable to real-world design optimization problems which usually involve non-differentiable/ multimodal objective function and/or a mix of continuous, discrete, and integer design parameters.
2. Suitability to parallel computing environment: Because MOEA is a population-based search algorithm, all design candidates in each generation can be evaluated in parallel by using the simple master-slave concept. Parallel efficiency is also very high, if objective function evaluations consume most of central processing unit (CPU) time. Aerodynamic optimization using CFD is a typical case.
3. Simplicity in coupling CFD codes: As MOEA uses only objective/constraint function values of design candidates, MOEA does not need substantial modification or sophisticated interface to the CFD code. If an all-out re-coding were required to every optimization problem, like the adjoint methods, extensive validation of the new code would be necessary every time. MOEA can avoid such troubles.

These features are essential for knowledge extraction from the present multiobjective optimization problem. Therefore, the MOEA presented in the next section is used to obtain the Pareto-optimal solutions of the present flapping motion design optimization problem.

As MOEA originally simulated natural evolution, traditional MOEA treats design parameters represented by binary numbers. However, for real design parameter optimizations such as the present aerodynamic optimization problem, it is more straightforward to use real numbers. Thus, the present design parameters h, k, α_0, α_1, and ϕ are represented by real numbers.

A flowchart of the present MOEA is illustrated in Fig. 5. The population size is kept at 32 and the maximum number of generations is set to fifty. The initial population is generated randomly so that the initial population covers the entire design space presented in Table 1.

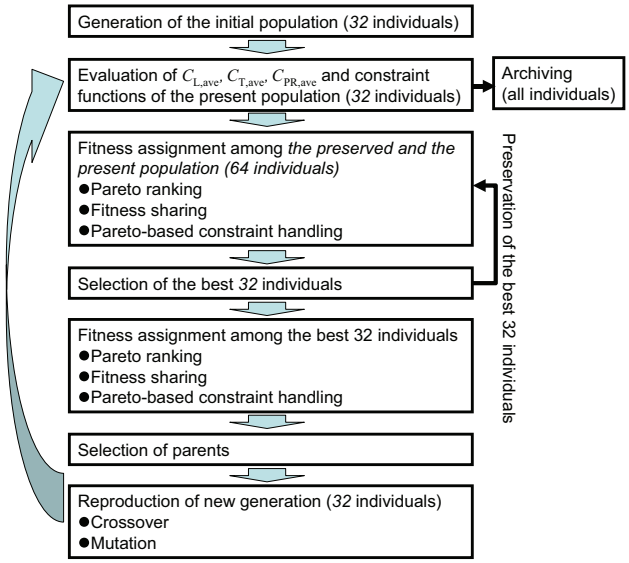

Fig. 5 Flowchart of the present MOEA.

Values of the present objective and constraint functions C_L, C_T, and C_{PR} of each design candidate are evaluated through CFD and fitness of each design candidate is computed according to Pareto-ranking, fitness sharing, and Pareto-based constraint handling [20] based on its objective function and constraint function values. Here, Fonseca and Fleming's Pareto-based ranking method and fitness sharing method [21] are used for Pareto-ranking where each individual is assigned a rank according to the number of individuals dominating it. In Pareto-based constraint handling, rank of feasible designs is determined by Pareto-ranking based on the objective function values while rank of infeasible designs is determined by Pareto-ranking based on the constraint function values.

Parents of new generations are selected through a roulette selection [22] from the best 32 individuals among the present generation and the best 32 individuals in the previous generation.

New generations are reproduced through crossover and mutation operators. Crossover is an operator which combines the genotypes of the selected parents and produces new individuals with the intent of improving the fitness value of the next generation. Here, the blended crossover [23] where α of 0.5 is used for crossover between the selected solutions. Mutation is applied to the design parameters of the new generation to maintain diversity. Here, mutation takes place at a probability of 20% and then adds a random disturbance to the corresponding gene up to 10% of the given range of each design parameter.

An evaluation process at each generation is parallelized using the master–slave concept, where the grid generations and the flow calculations associated to the individuals of a generation are distributed into 32 processing elements of the JAXA ISAS NEC SX-6 computing system. This makes the corresponding turnaround time almost 1/32 because the CPU time used for MOEA operators are negligible. Total turn around time of the present optimization is roughly nine hours.

V. Data Mining

If an optimization problem has two objective functions, the tradeoff relation between them as well as the effect of each design parameter can be easily understood through a two-dimensional plotting. On the other hand, understanding the tradeoff relations and effect of design parameters involving three or more objective functions is not so straightforward. Kohonen's SOM [7] is used to analyze the Pareto-optimal solutions in the present study.

SOM is an artificial neural network where all the solutions are aligned on a grid according to Kohonen algorithm so that neighboring nodes are similar to each other. Mostly, SOM is used for nonlinear projections of input data in three or higher dimensional space onto two-dimensional space to extract knowledge implicit in data such as attributes and features.

A software package called Viscovery SOMine plus 4.0 (http://www.viscovery.net/) produced by Eudaptics GmbH is used. Although SOMine is based on the general SOM concept and algorithm, it employs an advanced variant of unsupervised neural networks, i.e. Kohonen's Batch SOM, which is a more robust approach owing to its mediation over a large number of learning steps.

The Pareto-optimal solutions distributed in the present three-dimensional objective function space (C_L maximization, C_T maximization, and C_{PR} minimization) are mapped into nodes on a two-dimensional grid according to the similarity in terms of the objective function values. Here, map size is 51 $\times$ 41 (2070 nodes) and number of training is 45 with tension of 0.5. These values are automatically determined by the SOMine. It should be noted that direction and Euclidean distance in the objective function space are lost on the SOM. Then the two-dimensional map colored according to each objective function, each design parameter, propulsion efficiency, and Strouhal number are compared for the knowledge acquisition from the present problem.

VI. Results and Discussion

The Pareto-optimal flapping motions (shown by spheres) and all the other solutions (shown by circles) obtained by the present optimization are plotted in the three-dimensional objective function space (Fig. 6). The Pareto-optimal flapping motions are all optimal in the sense that no other solutions in the search space are superior to them when all objectives are considered. Distribution of the Pareto-optimal solutions visualizes tradeoff among the maximization of the averaged lift and thrust and minimization of the averaged required power while it is very difficult to understand effect of each design parameter on the tradeoff in the three-dimensional scatter plot. In the first subsection, flow mechanism of the extreme Pareto-optimal flapping motions, i.e. lift-maximum, thrust-maximum, required-power-minimum designs (presented in Table 3) is investigated. Then, in the next subsection, the Pareto-optimal solutions are analyzed with SOM to obtain knowledge from all Pareto-optimal solutions.

A. Analyses of the Extreme Pareto-optimal Solutions

1. Flapping Motion for Maximum Thrust

Pressure coefficient distribution around the flapping airfoil for maximum thrust is shown in Fig. 7. This figure indicates that the upstroke produces a strong vortex separated from the leading edge on the lower surface to generate large thrust and the downstroke produces another strong vortex separated from the leading edge on the upper surface for large thrust. While this flapping motion produces thrust in both upstroke and downstroke, averaged lift is small because the vortex generated in upstroke produces negative lift.

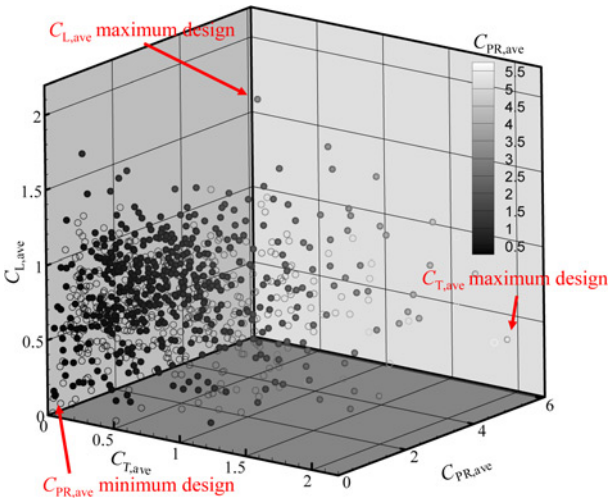

Fig. 6 Evaluated flapping motions (circles) and obtained Pareto-optimal solutions (spheres) plotted in the objective function space.

Table 3 Objective functions and design variable values of the extreme Pareto-optimal solutions

	Maximum thrust flapping	Maximum lift flapping	Minimum required power flapping
$C_{T,ave}$	2.09	0.77	0.03
$C_{L,ave}$	0.42	1.97	0.13
$C_{PR,ave}$	5.42	3.27	0.09
Reduced frequency k	0.88	0.80	0.46
Plunge amplitude h	2.10	2.06	1.88
Pitch amplitude α_1	38.2 [deg]	34.9 [deg]	37.7 [deg]
Pitch offset α_0	3.53 [deg]	21.2 [deg]	1.18 [deg]
Phase shift ϕ	94.0 [deg]	90.4 [deg]	85.5 [deg]

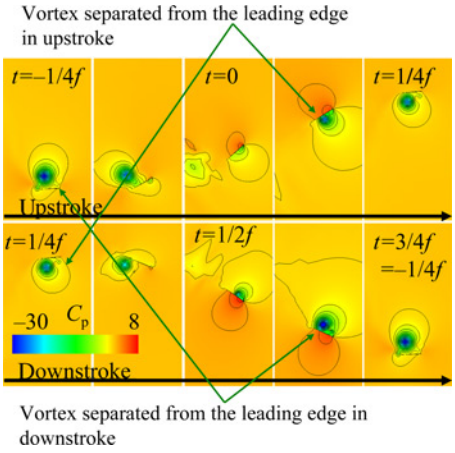

Fig. 7 Pressure coefficient distribution around the thrust maximum flapping motion.

Corresponding time histories of vertical position, pitch angle, effective angle of attack, lift, thrust, and required power coefficients of the maximum thrust flapping motion are presented in Fig. 8. This figure shows that flapping motion for maximum thrust has large absolute effective angle of attack to produce strong vortex separated from the leading edge in both downstroke and upstroke.

Reduced frequency, and plunge amplitude reached the upper boundary of the present design space to produce strong vortices. Because the flapping motion for maximum thrust needs to create thrust in both downstroke and upstroke, the flapping motion and corresponding flow became symmetric. As a result, the pitch offset of this motion became almost zero.

2. Flapping Motion for Maximum Lift

Pressure coefficient distribution around the flapping airfoil for maximum lift is presented in Fig. 9. During the upstroke motion, the airfoil does not generate any large vortex as it would produce negative lift. On the other hand, during the downstroke, the airfoil generates two vortices; one separated from the leading edge and one separated from the trailing edge. It is estimated that as the vortex separated from the trailing edge does not contribute to thrust, the flapping motion for maximum thrust did not generate it.

Corresponding time histories of vertical position, pitch angle, effective angle of attack, lift, thrust, and required power coefficients of the maximum lift flapping motion are presented in Fig. 10. The effective angle of attack is almost zero in upstroke while it is more than 40 degrees in downstroke. As a result, lift maximum flapping motion generates very large lift in downstroke while it generates small thrust and small negative lift in upstroke.

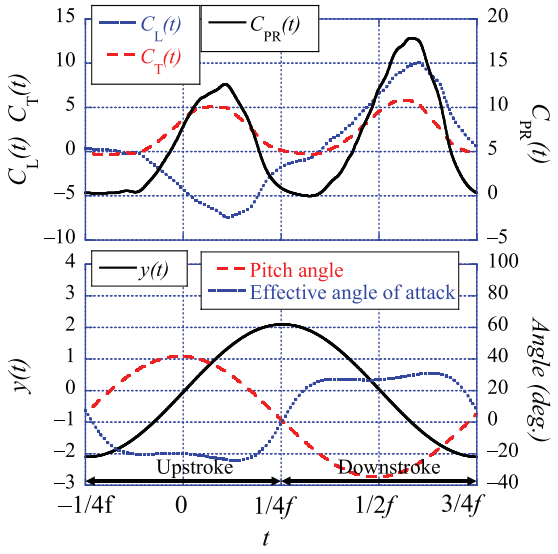

Fig. 8 Time histories of position, pitch angle, effective angle of attack, and the aerodynamic coefficients of the thrust maximum flapping motion.

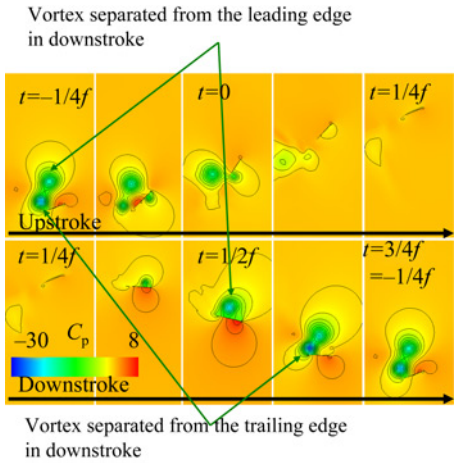

Fig. 9 Pressure coefficient distribution around the lift maximum flapping motion.

The flapping motion for maximum lift had large reduced frequency, and large plunge amplitude to produce strong vortices. To create strong vortex only in downstroke, the flapping motion for maximum lift had substantial pitch offset. The pitch amplitude was optimum at 35 degrees in the present design problem as the larger pitch amplitude reduces lift component and generates negative thrust component produced by the vortices in downstroke.

3. Flapping Motion for Minimum Required Power

Pressure coefficient distribution around the flapping airfoil for minimum required power is presented in Fig. 11. In contrast to the previous extreme flapping motions, this flapping motion does not create any strong vortex in both downstroke and upstroke to minimize the required power.

Corresponding time histories of vertical position, pitch angle, effective angle of attack, lift, thrust, and required power coefficients of the minimum required power flapping motion are presented in Fig. 12. This figure confirms that this flapping motion maintain almost zero effective angle of attack in both upstroke and downstroke.

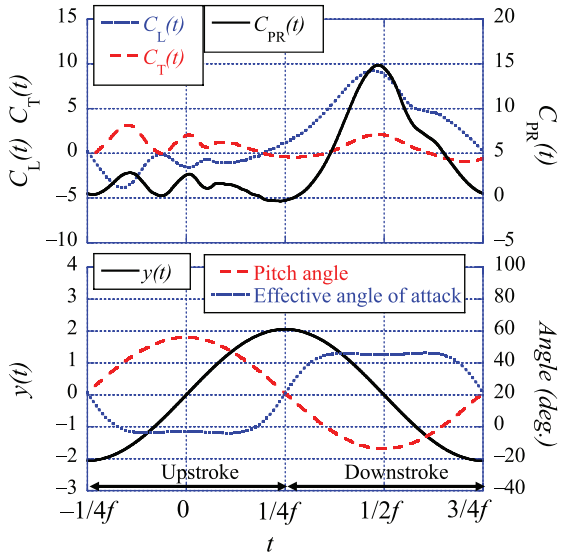

Fig. 10 Time histories of position, pitch angle, effective angle of attack, and the aerodynamic coefficients of the lift maximum flapping motion.

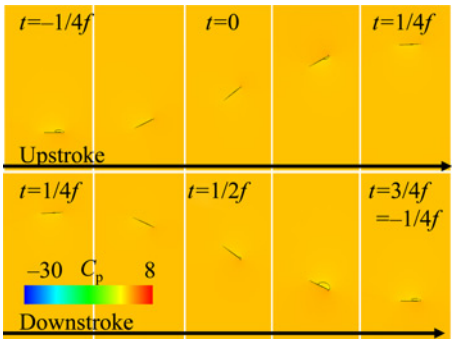

Fig. 11 Pressure coefficient distribution around the required power minimum flapping motion.

Because the flapping motion for minimum required power needs to not create any vortex in both downstroke and upstroke, the flapping motion and corresponding flow became symmetric. As a result, pitch offset became almost zero.

B. Data Mining Using SOM

Figure 13 is the obtained map using SOM where each node is colored according to each objective function value. It should be noted that as the number of Pareto-optimal solutions is 560 and the number of nodes of SOM is 2070, each Pareto-optimal solution is represented by one or more nodes on the map as shown in the figure. For example, four nodes located at the lower left corner represent $C_{L,ave}$ maximum design while one node located at the upper right corner represents $C_{PR,ave}$ minimum design. This figure shows flapping motions for smaller required power are mapped on the right side of the map. Flapping motions for larger lift are mapped on the lower left and lower right corners where flapping motions mapped on the lower left corner require large power while those mapped on the lower right corner require smaller power. The flapping motions for larger thrust are mapped on the left hand side.

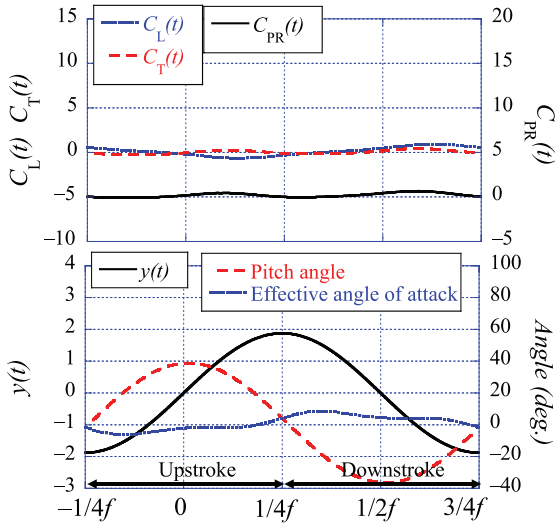

Fig. 12 Time histories of position, pitch angle, effective angle of attack, and the aerodynamic coefficients of the required power minimum flapping motion.

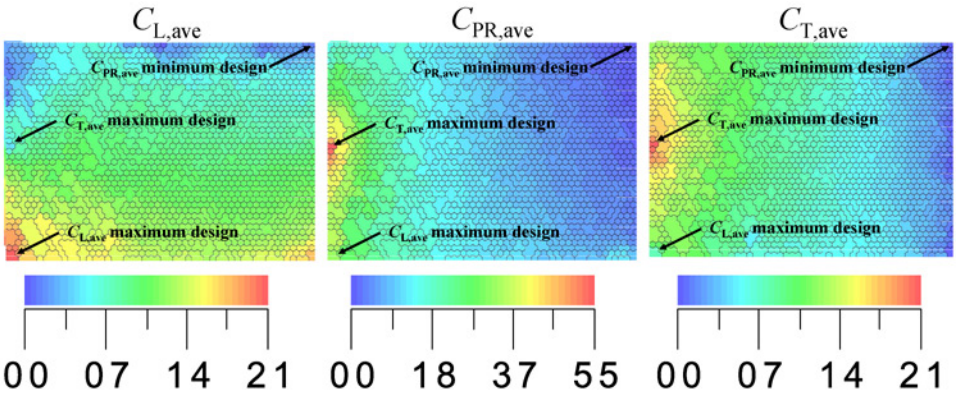

Fig. 13 SOM colored according to each objective function.

These results indicate the tradeoff between the three objectives exists and thus there is no solution that optimizes all three objectives simultaneously. This figure also indicates that maximizing thrust requires more power than maximizing lift.

The same map colored according to propulsive efficiency and Strouhal number is presented in Fig. 14. According to the research by Taylor et al. [24], flying animals such as birds, bats and insects in cruise flight operate within a narrow range of Strouhal number between 0.2 and 0.4. Also, Young [25] demonstrated some Navier–Stokes computations to show propulsive efficiency has a peak around a Strouhal number of 0.2. Strouhal number of the obtained flapping motions is consistent with these results.

Distribution of propulsive efficiency shows that flapping motions for maximum propulsive efficiency have small lift. This result is understandable because generation of lift does not contribute to the propulsive efficiency, which is determined by thrust divided by the required power. The propulsive efficiency was maximized at a certain point between maximization of thrust and minimization of required power. Figure 14 also shows that *St* becomes smaller as required power becomes smaller while it becomes larger as thrust or lift becomes larger.

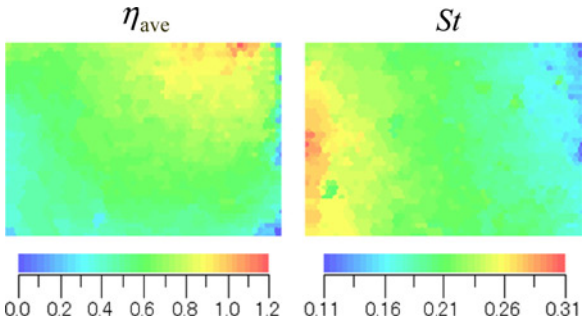

Fig. 14 SOM colored according to propulsive efficiency and Strouhal number.

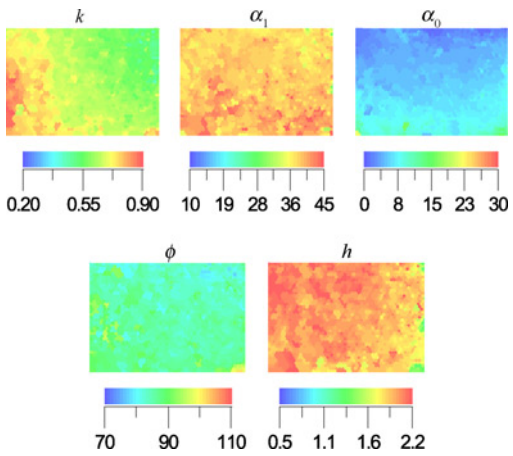

Fig. 15 SOM colored according to each design parameter.

The same SOM colored according to each design parameter value is presented in Fig. 15. Color range of the map corresponds to the present design range. Comparison between Figs. 13 and 15 gives additional knowledge on the present design optimization problem:

1. Phase shift between plunging and pitch angle cycles of the obtained Pareto-optimal solutions are almost 90 degrees. This result is consistent with previous researches on flapping motion such as [3] where efficiency became high when pitch leads plunging by about 90 degrees.
2. Pitch angle offset of most Pareto-optimal flapping motions is almost zero except for the flapping motions for high lift. This is understandable as the thrust maximum and required power minimum flapping motion is symmetric while lift maximum flapping motion generates lift only in downstroke.
3. Reduced frequency seems to be a tradeoff parameter between minimization of required power and maximization of lift or thrust where smaller frequency leads to smaller required power.
4. Plunge amplitude of most Pareto-optimal flapping motions reached the upper limit of the present design space. This fact indicates that larger plunge amplitude is preferable when two-dimensional flow is assumed. However, in real flapping wing design, the plunge amplitude is restricted by span length and angle of the flapping wing along the flap arc.
5. Pitch angle amplitude of the most Pareto-optimal solutions distributes between 35 and 45 degrees, which indicates that certain level of pitch angle amplitude is optimum for high performance flapping motion. This figure also indicates that better solutions may have been found if the search space was wider because 45 degrees is upper limit of the present search space of α_1.

This knowledge is consistent with that obtained in the previous subsection.

VII. Conclusions

The MODE framework has been applied to a multiobjective aerodynamic design optimization problem of a flapping airfoil to obtain aerodynamic knowledge for practical flapping-wing MAV design. To explore the design problem, the Pareto-optimal solutions obtained by a multiobjective evolutionary algorithm were analyzed with the self-organizing map and the time histories of lift, thrust, and required power coefficients and corresponding pressure coefficient distribution of the extreme Pareto-optimal solutions were discussed.

Discussion on the aerodynamics of the extreme Pareto-optimal solutions gave us insight into flow mechanism for thrust maximization, lift maximization, and required power minimization:

1. Aerodynamic forces produced by a flapping airfoil are largely owing to vortex generation both from the leading edge and the trailing edge.
2. Flapping motion for maximum thrust generates large thrust and large lift in downstroke and large thrust and large negative lift in upstroke.
3. Flapping motion for maximum lift generates large positive lift in downstroke and small thrust and lift in upstroke.
4. Flapping motion for minimum required power generates small thrust and lift in both upstroke and downstroke.

Analysis of the objective function values of the Pareto-optimal solutions using SOM showed tradeoff between thrust maximization, lift maximization and required power minimization. Analysis of the design variables of the Pareto-optimal solutions using SOM leaded to some knowledge on aerodynamic flapping mechanism:

1. Phase shift between plunging and pitch angle cycles of the obtained Pareto-optimal solutions are almost ninety degrees.
2. Pitch angle offset of most Pareto-optimal flapping motions is almost zero except for the flapping motions for high lift.
3. Reduced frequency is a tradeoff parameter between minimization of required power and maximization of lift or thrust where smaller frequency leads to smaller required power.
4. Larger plunge amplitude is preferable when two-dimensional flow is assumed.
5. Certain level of pitch angle amplitude is optimum for high performance flapping motion.

The present result ensured that the MODE framework coupled with CFD is useful approach for real-world design optimization problems. Although the present demonstration was MAV design for Mars exploration, the aerodynamic knowledge extracted from the present study should be useful for designers of flapping-wing MAV for Earth air as long as Reynolds number and cruising speed is almost same.

References

[1] Garrick, I. E., "Propulsion of a Flapping and Oscillating Airfoil," NACA Report 567, 1936.

[2] Tuncer, I. H., and Platzer, M. F., "Thrust Generation Due to Airfoil Flapping," *AIAA Journal,* Vol. 34, No. 2, 1995, pp. 324–331.
doi: 10.2514/3.13067

[3] Isogai, K., Shinmoto, Y., and Watanabe, Y., "Effects of Dynamic Stall on Propulsive Efficiency and Thrust of Flapping Airfoil," *AIAA Journal*, Vol. 37, No. 10, 1999, pp. 1145–1151.
doi: 10.2514/2.589

[4] Tuncer, I. H., and Kaya, M., "Optimization of Flapping Airfoils for Maximum Thrust and Propulsive Efficiency," *AIAA Journal*, Vol. 43, No. 11, 2005, pp. 2329–2336.
doi: 10.2514/1.816

[5] Anderson, J. M., Streitlien, K., Barrett D. S., and Triantafyllou, M. S., "Oscillating Foils of High Propulsive Efficiency," *Journal of Fluid Mechanics,* Vol. 360, No. 1, 1998, pp. 41–72.

[6] Deb, K., *MultiObjective Optimization Using Evolutionary Algorithms,* John Wiley & Sons, Chichester, UK, 2001.

[7] Kohonen, T., *Self-Organizing Maps,* 2nd ed., Springer Verlag, Heidelberg, Germany, 1997.

[8] Donald, R. J., Matthias, S., and William, J. W., "Efficient Global Optimization of Expensive Black-Box Function," *Journal Global Optimization,* Vol. 13, 1998, pp. 455–492.

[9] Obayashi, S., Jeong, S., and Chiba, K., "Multi-Objective Design Exploration for Aerodynamic Configurations," AIAA Paper 2005-4666, AIAA, 2005.

[10] Colozza, A., Landis, G., and Lyons, V., "Overview of Innovative Aircraft Power and Propulsion Systems and Their Applications for Planetary Exploration," NASA TM-212459, 2003.

[11] Michelson, R. C., "Novel Approaches to Miniature Flight Platforms," *Journal of Engineering,* Vol. 218, No. 6, 2004, pp. 363–373.
[12] Chorin, A. J., "A Numerical Method for Solving Incompressible Viscous Flow Problems," *Journal of Computational Physics*, Vol. 2, 1967, pp. 12–26.
doi: 10.1016/0021-9991(67)90037-X
[13] Jameson, A., "Time Dependent Calculations Using Multigrid, with Applications to Unsteady Flows Past Airfoils and Wings," AIAA Paper 1991-1596, AIAA, 1991.
[14] Roe, P. L., "Approximate Riemann Solvers, Parameter Vectors, and Difference Schemes," *Journal of Computational Physics*, Vol. 43, 1981, pp. 357–372.
doi: 10.1016/0021-9991(81)90128-5
[15] van Leer, B., "Towards the Ultimate Conservative Difference Scheme. A Second-Order Sequel to Godunov's Method," *Journal of Computational Physics,* Vol. 32, 1979, pp. 101–136.
[16] Yoon, S., and Jameson, A., "Lower-Upper Symmetric-Gauss-Seidel Method for the Euler and Navier–Stokes Equations," *AIAA Journal,* Vol. 26, No. 9, 1988, pp. 1025–1026.
doi: 10.2514/3.10007
[17] Ito, T., Fujii, K., and Hayashi, K., "Computations of Axisymmetric Plug-Nozzle Flowfields: Flow Structures and Thrust Performance," *Journal of Propulsion and Power*, Vol. 18, No. 2, 2002, pp. 254–260.
doi: 10.2514/2.5964
[18] Kawai, S., and Fujii, K., "Analysis and Prediction of Thin-Airfoil Stall Phenomena with Hybrid Turbulence Methodology," *AIAA Journal*, Vo. 43, No. 5, 2005, pp. 953–961.
doi: 10.2514/1.11672
[19] Fujimoto, K., and Fujii, K., "Computational Aerodynamic Analysis of Capsule Configurations toward the Development of Reusable Rockets," *Journal of Spacecraft and Rockets*, Vol. 43, No. 1, 2006, pp. 77–83.
doi: 10.2514/1.13377
[20] Oyama, A., Shimoyama, K., and Fujii, K., "New Constraint-Handling Method for Multi-objective Multi-Constraint Evolutionary Optimization," *Transactions of the Japan Society for Aeronautical and Space Sciences*, Vol. 50, No. 167, 2007, pp. 56–62.
doi: 10.2322/tjsass.50.56
[21] Fonseca, C. M., and Fleming, P. J., "Genetic Algorithms for Multiobjective Optimization: Formulation, Discussion and Generalization," *Proceedings of the 5th International Conference on Genetic Algorithms*, edited by S. Forrest, Morgan Kaufmann, San Mateo, CA, 1993, pp. 416–423.
[22] Goldberg. D. E., *Genetic Algorithms in Search, Optimization and Machine Learning*, Addison-Wesley Longman, Reading, MA, 1989.
[23] Eshelman, L. J., and Schaffer, J. D., "Real-Coded Genetic Algorithms and Interval Schemata," *Foundations of Genetic Algorithms 2*, edited by L. D. Whitley, Morgan Kaufmann, San Mateo, CA, 1993, pp. 187–202.
[24] Taylor, G. K., Nudds, R. L., and Thomas, A. L. R., "Flying and Swimming Animals Cruise at a Strouhal Number Tuned for High Power Efficiency," *Nature*, Vol. 425, 2003, pp. 707–711.
doi: 10.1038/nature02000
[25] Young, J., "Numerical Simulation of the Unsteady Aerodynamics of Flapping Airfoils," Ph.D. Dissertation, School of Aerospace, Civil and Mechanical Engineering, The University of New South Wales, Australian Defense Force Academy, Sydney, Australia, 2005.

Kelly Cohen
Associate Editor